

Supporting Information for the manuscript entitled

Processes controlling the thermal regime of salt marsh channel beds

by Kevan B. Moffett, Scott W. Tyler, Thomas Torgersen,
Manoj Menon, John S. Selker, and Steven M. Gorelick.

This *Supporting Information* includes seven pages, with four figures.

Summary: a listing of equipment used, elaboration on detection of diffuse groundwater discharge, and details of interpretation of data by *Cho et al.*

Field instrumentation

The following equipment was used in data collection for this study.

- Distributed Temperature Sensing unit: DTS Model N4385
Agilent Technologies, Germany
- Fiber-optic cable: 50/125 multimode quartz glass optical fiber (0.6-mm) with steel and Kevlar wrap and PVC jacket, E-2000 cable-end connectors and 8-degree polished angle-cut terminations
Kaiphone Technologies Co. Limited, Taiwan
- Temperature loggers: HOBO® Water Temp Pros
Onset Computer Corporation, Bourne, MA
- Pressure-temperature loggers: Aquistar® PT2X Submersible Smart Sensors
Instrumentation Northwest, Kirkland, WA
- Weather station: HOBO® Weather Station
Onset Computer Corporation, Bourne, MA

Elaboration on detection of diffuse groundwater discharge

This *Supporting Information* provides, in more detail, the evidence for our assertion in the *Results and Discussion* section of the main manuscript that we detected diffuse groundwater discharge throughout the channels during both high and low tides. As in the main manuscript, we divide the discussion into two primary arguments drawn from two different time periods within our data.

Case 1: Bed temperature decline while beneath night-time ebb tide

The declining temperatures measured by the DTS during the ebb of the night-time high tide are apparent in Figure S1. To emphasize the difference between the DTS bed temperatures and the temperature of the tidal water, the value plotted is bed temperature minus surface water temperature. Tidal waters were of a constant temperature while within the channel during this period (17.53 ± 0.04 °C, median $\pm 1\sigma$).

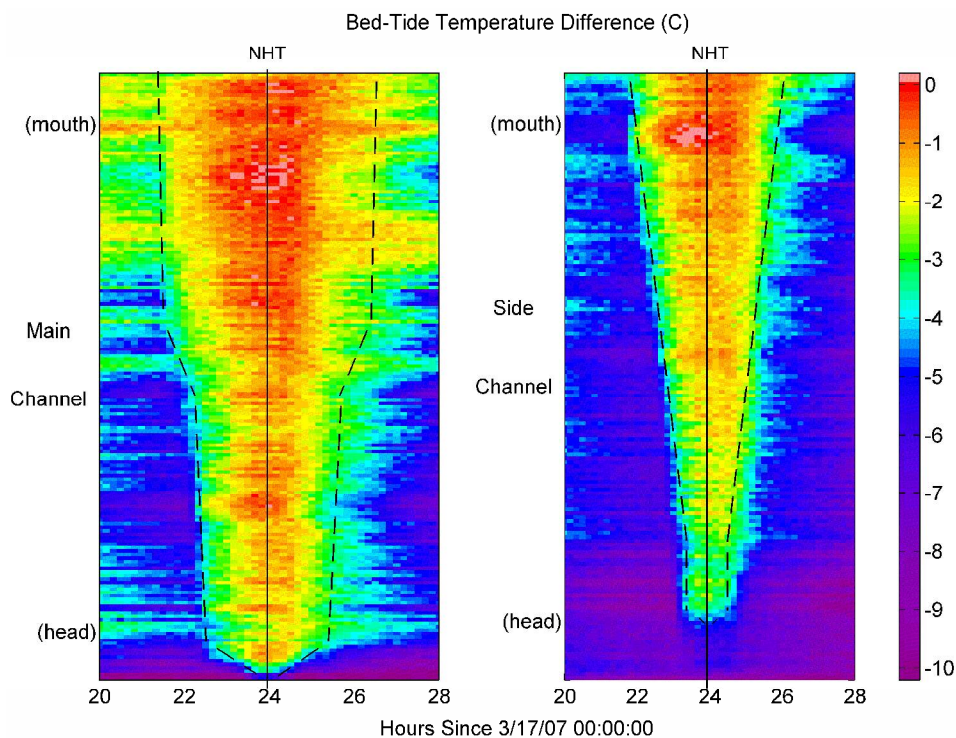


Figure S1: Temperature difference between NHT channel bed and warmer tidal waters. Solid lines mark the time of the night-time high tide; dashed lines enclose the approximate duration of flooding.

To further highlight the temperature decline measured during this period at locations that remained insulated by warm overlying surface water, we selected one segment of DTS data as an example: this segment was located at the channel junction (at the main and side channel mouths) and selected since it was flooded for the longest duration. Temperatures from this location are plotted in Figure S2. The steady decline in bed temperatures, while still covered by warm tidal waters, is evident. The temperature declines throughout the channels are explained by cold groundwater discharge since cooling by radiation and conduction can be ruled out, as explained in the main text.

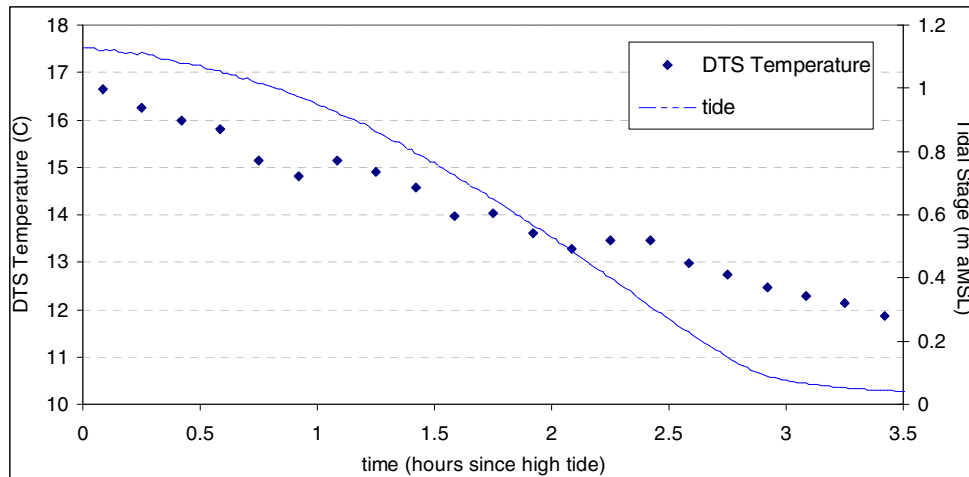


Figure S2: DTS temperature history at the channel junction (mouths) and coincident tidal stage following NHT.

Case 2: Bed temperatures below air temperature while shaded/after sunset

From the time just prior to the sunset of day one, when the low angle of the sun put the channels in shade, until three hours after sunset, when the night-time flood tide occurred, the DTS measured temperatures well below air temperature at some locations. This time period is called out by the black box in Figure S3; Figure S3 presents the temperature difference between air and the channel bed (air temperature – bed temperature).

We selected one location near the head of the side channel, marked on Figure S3 with an arrow, for which we present in Figure S4 a more detailed picture of the data. The warmer air temperatures during this period permitted us to rule out conductive heat loss; we also ruled out attributing this magnitude of temperature decrease to radiative or evaporative cooling, as explained in the main text. In the absence of these factors, the

decline of bed temperatures below that of the air, at all locations shown in blue within the box of Figure S3, is conclusively attributed to cold groundwater exfiltration. Other locations likely experience groundwater discharge but are not conclusively detectable in this example.

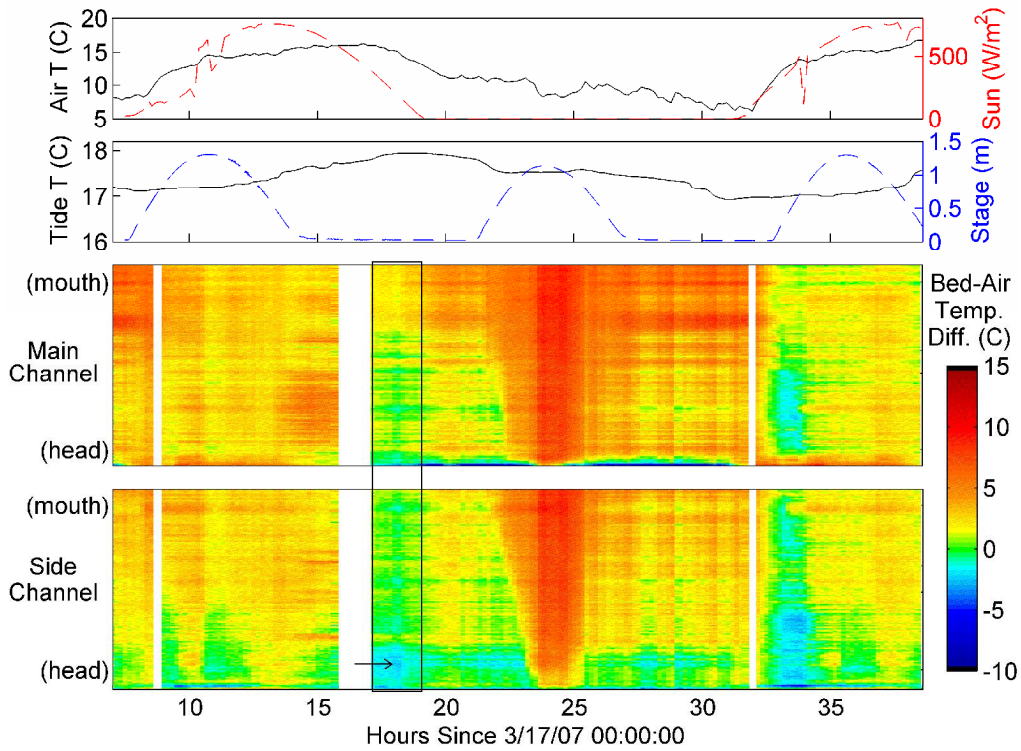


Figure S3: Temperature difference between channel bed (DTS data) and air. Black box highlights period of channel in shade prior to sunset. Conductive heat loss from channel bed is ruled out for values < 0 , in blue.

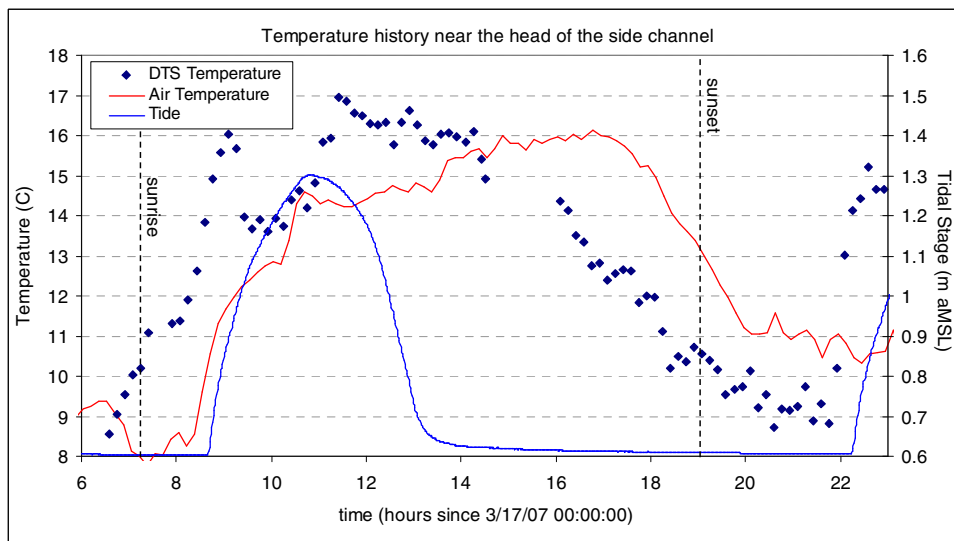


Figure S4: DTS temperature history at one location near the head of the side channel registering temperatures significantly below air temperature during low tide.

Details of interpretation of data by *Cho et al.*

In the main text we compared our data on inland-decreasing temperature gradients in salt marsh tidal channels to data published by *Cho et al.* for intertidal mudflats; theirs was the only prior study on horizontal temperature gradients in intertidal sediments of which we were aware. The comparison of salt marsh-channel and mudflat data provided context for our study and emphasized the importance of topography, notably the relief of incised tidal channels, in modifying the relative influences on the benthic thermal regime of groundwater advection, solar radiation, heat conduction from/to the air, and the tidal thermal blanket effect.

We direct the reader to Figure 4 of the paper by *Cho et al.* for an illustration of temperature trends detected in mudflat sediments. These trends can be compared to the lines in Figure 4 of our manuscript, which show temperature trends along salt marsh channel beds. We point out that *Cho et al.* focused their discussion on a different aspect of their data and omitted discussion of intertidal sediment temperature trends in their manuscript; our study seems to be the first to examine this phenomenon in detail. We note that the trends of *Cho et al.* are based on data at 2-4 locations at three times; our trends are based on data from 331 locations at 238 times.

The data by *Cho et al.* were somewhat difficult to interpret as potential end-member temperatures were not reported; much of the relevant information could be inferred from the paper's Figure 2, however. We present our interpretation of their data here, to better explain our conclusions regarding the effects of the tidal thermal blanket throughout the intertidal zone and the relative prominence of radiative warming and lack of groundwater cooling in the mudflats of *Cho et al.*.

We interpret the relatively invariant, high tide-coincident temperatures (~ 19 °C in spring) in Figure 2a (*Cho et al.*) as having their source in tidal surface waters. This conclusion is supported by the regularity of the temperatures, their consistency during higher-high tides, and the coincident destruction of vertical temperature stratification in the near-surface sediments. We infer that the large temperature spikes at shallow depths during daytime low tides in Figures 2a, 2b and 3c (*Cho et al.*) are caused by intense

radiative heating, which strongly dominates over the apparent night-time/low tide cooling also shown in these figures. The result of the intense radiative heating is that the average temperature of locations experiencing prolonged exposure is warmer than the ~19 °C surface water, providing the warm end-member for the trends plotted by *Cho et al.* in Figure 4a/b. Decreased autumnal solar warming and, presumably, colder air temperatures (Figure 2c, *Cho et al.*) result in the reversed gradient of Figure 4c (*Cho et al.*) as the cooler tidal end-member becomes a warmer end-member, instead, during this season. In all seasons, the surface water provides a temperature anchor for locations infrequently exposed. The autumn gradient reversal highlights the importance of solar heating in the thermal balance of the mudflat system. Since solar heating was not found to be as significant a contributor in salt marsh channels and groundwater temperatures are relatively constant, we expect no such reversal in salt marsh systems where surface water is consistently warmer than ground water.

We also note that Figure 2 by *Cho et al.* suggests variably saturated mudflat conditions because the wide variation in temperature at 40-cm depth, from 6-7 °C (winter) to 23 °C (summer), is not typical of groundwater. We expect that the necessarily shallow hydraulic gradient of very low-relief, unconfined intertidal mudflats does not produce enough groundwater discharge to overcome the strong solar warming of exposed sediments, again in contrast to the salt marsh system.

Cho, Y. K.; Kim, T. W.; You, K. W.; Park, L. H.; Moon, H. T.; Lee, S. H.; Youn, Y. H.
Temporal and spatial variabilities in the sediment temperature on the Baeksu tidal flat, Korea. *Estuar. Coast. Shelf Sci.* **2005**, *65*, 302-308.